

Foveal pit morphological changes in asymptomatic carriers of the G11778A mutation with Leber's hereditary optic neuropathy

Xin-Ting Liu, Mei-Xiao Shen, Chong Chen, Sheng-Hai Huang, Xi-Ran Zhuang, Qing-Kai Ma, Qi Chen, Fan Lu, Yi-Min Yuan

School of Ophthalmology and Optometry, the Eye Hospital, Wenzhou Medical University, Wenzhou 325027, Zhejiang Province, China

Correspondence to: Yi-Min Yuan. School of Ophthalmology and Optometry and Eye Hospital, Wenzhou Medical University, 270 Xueyuan Road, Wenzhou 325027, Zhejiang Province, China. yuanyimin1226@hotmail.com

Received: 2019-12-03 Accepted: 2020-03-12

Abstract

• **AIM:** To investigate the foveal pit morphology changes in unaffected carriers and affected Leber's hereditary optic neuropathy (LHON) patients with the G11778A mutation from one family.

• **METHODS:** This study was a prospective cross-sectional study. Both eyes from 16 family members (age from 9 to 47y) with the G11778A mutation were analyzed and compared with 1 eye from 20 normal control subjects. Eleven family members with the G11778A mutation but without optic neuropathy were classified as unaffected carriers ($n=22$ eyes). Five family members ($n=10$ eyes) expressed the LHON phenotype and were classified as affected patients. Retinal images of all the subjects were taken by optical coherence tomography (OCT), and an automatic algorithm was used to segment the retina to eight layers. Horizontal and vertical OCT images centered on the fovea were used to measure intra-retinal layer thicknesses and foveal morphometry.

• **RESULTS:** Thicker foveal thickness, thinner foveal pit depth, and flatter foveal slopes were observed in unaffected carriers and affected LHON patients (all $P<0.001$). Further, the slopes of all four sectors in the LHON were flatter than those in the unaffected carriers (all $P<0.001$). Compared with the control group, affected LHON patients had a thinner retinal nerve fiber layer (RNFL), ganglion cell layer and inner plexiform layer (GCL+IPL), and total retina (all $P<0.01$). The retinal nerve fiber layer (RNFL) of affected patients was 38.0% thinner than that of controls while the GCL+IPL was 40.1% thinner.

• **CONCLUSION:** The foveal pit morphology shows changes in both unaffected carriers and affected patients. RNFL and GCL+IPL are thinner in affected LHON patients but not in unaffected carriers.

• **KEYWORDS:** foveal pit morphology; Leber's hereditary optic neuropathy; asymptomatic carriers; G11778A

DOI:10.18240/ijo.2020.05.11

Citation: Liu XT, Shen MX, Chen C, Huang SH, Zhuang XR, Ma QK, Chen Q, Lu F, Yuan YM. Foveal pit morphological changes in asymptomatic carriers of the G11778A mutation with Leber's hereditary optic neuropathy. *Int J Ophthalmol* 2020;13(5):766-772

INTRODUCTION

Leber's hereditary optic neuropathy (LHON) is a maternally inherited eye disease usually leading to bilateral loss of central vision without pain in healthy young adults^[1-3]. It is associated with mitochondrial DNA (mtDNA) mutations, and over 95% of LHON case mutations occur at three-point positions: G3460A, G11778A, and T14484C^[4-7]. These mutations affect the first site of the mitochondrial respiratory chain complex I and result in respiratory chain dysfunction^[8]. Only about 50% of males and about 10% of females who harbor the pathogenic mtDNA mutation develop the optic neuropathy, most individuals are unaffected and show no symptoms. A DNA test is often used to check if a family member has the mutation. We are interested in identifying structural parameters that might aid in the diagnosis of asymptomatic carriers.

Asymptomatic LHON carriers are defined as individuals lacking the full phenotypic expression of the disease^[9]. However, these unaffected carriers have the pathogenic LHON mutation, some fundus changes, dyschromatopsia, and visual field defects^[10]. Retinopathy is the main characteristic of LHON, indicated by swelling of the retinal nerve fiber layer (RNFL), and rapid loss of the papillomacular bundle is seen on fundus examination^[11-12]. Histopathologic studies show that the neuropathology of LHON is limited to the retinal ganglion cell

Table 1 Clinical characteristics of the study groups

Characteristics	Controls (n=20)	Unaffected carriers (n=11)	Affected LHON patients (n=5)
No. of eyes	20	22	10
Male/female	12/8	3/8	4/1
Age (y)	25.1±2.0	29.7±14.0	37.4±10.7
Age range (y)	24-32	9-45	19-47
Onset age (y)			16.8±2.95
Onset age range (y)			12-20
Disease duration (y)			20.6±11.15
Disease duration range (y)			1-28

LHON: Leber's hereditary optic neuropathy.

layer (GCL), while the retinal pigment epithelium (RPE) and photoreceptor layer are spared^[13-14].

Optical coherence tomography (OCT) is a noninvasive, noncontact imaging technique that provides cross-sectional images of the retina *in vivo*^[15]. OCT-associated software can assess foveal morphology and calculate the thicknesses of the macular intra-retinal layers^[16-18]. Changes in thickness of these layers in glaucoma and diabetic retinopathy have been reported^[19-21]. A few studies have used OCT to investigate the thickness of the RNFL surrounding the optic papilla in LHON patients^[22-24]. However, the characteristic field defect in LHON is a central scotoma^[25], and approximately 50% of the retinal ganglion cells (RGCs) are present in the macula. Therefore, evaluating structural changes in the macula is important. Our previous study investigated the three-dimensional thicknesses of four macular intraretinal layers in symptomatic and asymptomatic carriers of G11778A mutation with LHON; the nerve fiber layer, the GCL and the inner plexiform layer (IPL) were observed to be thin in symptomatic but not in asymptomatic carriers of G11778A mutation^[26]. Foveal pit morphology has not been assessed in symptomatic and asymptomatic carriers of G11778A mutation with LHON. Thus, the aim of this study was to investigate the foveal pit morphological changes in unaffected carriers and affected LHON patients with the G11778A mutation from one family and provide parameters to distinguish unaffected carriers from normal subjects.

SUBJECTS AND METHODS

Ethical Approval The study adhered to the tenets of the Declaration of Helsinki and was approved by the Ethics Committee of the Wenzhou Medical University [KYK(2015)9]. All subjects had been fully informed of the purpose and methods of the present study and provided written informed consent.

Subjects Sixteen patients from one family with the G11778A mutation were included in this study (Table 1). Eleven of them (age 9 to 45y, 3 males and 8 females) were unaffected carriers and five of them (age 19 to 47y, 4 males and 1 female) expressed the LHON phenotype. One eye each from 20 normal

subjects (age 24 to 32y, 12 males and 8 females) served as controls.

Ophthalmic examinations were conducted for all subjects and included best-corrected visual acuity (BCVA), slit-lamp biomicroscopy, indirect ophthalmoscopy, and optic nerve head photography. Exclusion criteria were the presence in one or both eyes of any retinal disease other than LHON, such as open-angle glaucoma and atrophic optic nerve caused by trauma or brain disease. Patients were classified based on clinical and genetic criteria. Subjects with the G11778A mutation were divided into two groups: unaffected carriers and affected LHON. The unaffected carriers were defined as members of the LHON family who carried the G11778A mutation but who had a normal visual ability (the BCVA≥20/20). All the affected LHON subjects in this study had a severe visual impairment with BCVA<20/200 in both eyes.

Instruments and Image Analysis All the measurements were obtained by a commercially available OCT instrument (RTVue100, Optovue, Inc., Fremont, CA, USA). The RTVue100 had an axial resolution of approximately 5 μm with a center wavelength of 840 nm and a bandwidth of 50 nm. Macular retinal images were acquired using the cross-line scan mode with an 8-mm scan length. Each OCT B-scan image consisted of 640 pixels (2 mm) in depth and 960 pixels (8 mm) in length. A mathematical model with Matlab software was used to determine foveal parameters. The boundaries of the internal limiting membrane (ILM) and RPE were first detected and used to obtain a profile of the total retinal thickness. Five landmarks of the fovea (Figure 1) were automatically identified by the software. The temporal and nasal rims of the fovea in the horizontal meridian (Figure 1A, 1E) and the inferior and superior rims in the vertical meridians had no slope. Similarly, the pit of the fovea (Figure 1C) had no slope. The maximum slopes of the temporal and nasal foveal walls in the horizontal meridian (Figure 1B, 1D) and of the inferior and superior walls in the vertical meridian were also determined. Based on these five landmarks, we extracted five prominent features of the foveal pit: foveal thickness, pit depth, diameter, maximum thickness, and foveal slope^[17,21].

Table 2 Foveal pit morphology in control group, unaffected carriers, and affected LHON patients

Parameters	Control	Unaffected carriers	LHON patients	<i>P</i> (ANOVA)	<i>P</i> (LSD_1/2)	<i>P</i> (LSD_1/3)	<i>P</i> (LSD_2/3)
Foveal thickness (μm)	214.73±13.90	235.36±21.65	247.29±26.47	<0.001	0.001	<0.001	0.124
Foveal pit depth (μm)	159.42±24.22	129.50±14.81	87.17±35.27	<0.001	<0.001	<0.001	<0.001
Foveal pit diameter (μm)	2217.77±211.45	2106.49±114.96	2129.02±340.79	0.214	0.089	0.278	0.780
Temporal max thickness (μm)	341.11±19.40	343.04±25.68	298.53±18.39	<0.001	0.777	<0.001	<0.001
Nasal max thickness (μm)	362.33±19.89	356.61±17.59	305.56±17.19	<0.001	0.316	<0.001	<0.001
Inferior max thickness (μm)	364.13±19.59	361.94±24.33	305.44±18.02	<0.001	0.739	<0.001	<0.001
Superior max thickness (μm)	369.86±20.42	360.99±21.20	309.26±20.27	<0.001	0.167	<0.001	<0.001
Temporal foveal slope (°)	10.27±2.46	7.99±2.58	3.72±1.80	<0.001	0.003	<0.001	<0.001
Nasal foveal slope (°)	11.08±2.50	8.53±2.47	3.86±1.92	<0.001	0.003	<0.001	<0.001
Inferior foveal slope (°)	12.54±2.49	10.13±2.28	4.92±1.77	<0.001	0.001	<0.001	<0.001
Superior foveal slope (°)	12.79±2.34	10.13±2.25	5.20±1.54	<0.001	<0.001	<0.001	<0.001

mean±SD

LSD_1/2: Fisher’s least significant difference *t*-test between control group and unaffected carriers; LSD_1/3: Fisher’s least significant difference *t*-test between control group and affected LHON patients; LSD_2/3: Fisher’s least significant difference *t*-test between unaffected carriers and affected LHON patients.

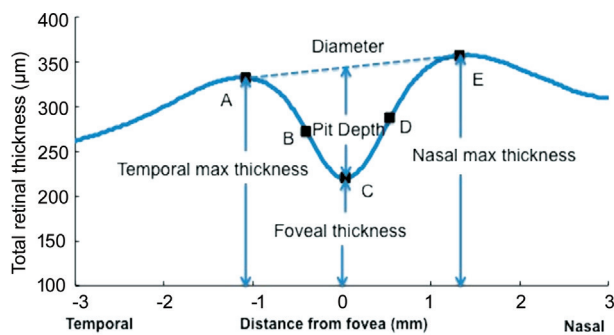


Figure 1 Foveal parameters in the horizontal meridian determined using a mathematical model with Matlab software A, E: A zero slope and indicate the peak of the temporal and nasal foveal rims; C: A zero slope and is the center of the foveal pit; B, D: The maximum slopes of the foveal wall. Similar points were identified for the vertical meridian.

Horizontal and vertical retinal OCT images centered on the fovea were acquired from all participants. An automatic segmentation algorithm combined with Matlab software (MathWorks, Inc., Natick, MA, USA) was used to segment the macular retinal images to eight layers (Figure 2), including 1) RNFL; 2) GCL+IPL; 3) inner nuclear layer (INL); 4) outer plexiform layer (OPL); 5) outer nuclear layer (ONL); 6) photoreceptor inner segment (IS) layer; 7) photoreceptor outer segment (OS) layer; 8) RPE. The details of this method have been described in previous studies^[16,18]. Each layer thickness profile consisted of 300 data points, and the average intra-retinal layer thickness also had a mean of 300 data points. The horizontal thickness profile was divided into temporal and nasal sectors, and the vertical thickness profile was divided into inferior and superior sectors.

Statistical Analysis The right eye of 20 normal subjects, and both eyes of unaffected carriers (22 eyes) and affected LHON patients (10 eyes) were analyzed. All data were expressed as means±standard deviations and analyzed with SPSS software (version 17.0, SPSS Inc., Chicago, IL, USA). Analysis of

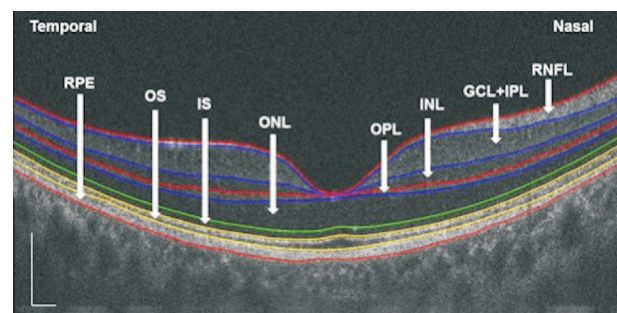


Figure 2 Segmentation of the macula retinal image into eight layers using an automatic segmentation algorithm combined with Matlab software.

variance (ANOVA) was used to analyze differences between the unaffected carriers and affected LHON patients compared with the control group. Independent sample *t*-tests were used to analyze differences between males and females among the unaffected carriers. *P*-values <0.05 were considered statistically significant.

RESULTS

The fovea was thicker and foveal pit depth was shallower in unaffected carriers and LHON patients compared to normal controls (both *P*<0.001, Table 2). The thickness profiles of the total retina in the central area were shallower in unaffected carriers and LHON patients compared to normal subjects (Figure 3). Compared to normal subjects, the maximum thicknesses in all four sectors were significantly smaller only in LHON patients, not in unaffected carriers (all *P*<0.001, Table 2). The foveal slopes in the temporal, nasal, inferior, and superior sectors were all flatter in both unaffected carriers and LHON patients compared to normal controls (all *P*≤0.003, Table 2). Further, the slopes of all four sectors in the LHON were flatter than those in the unaffected carriers (all *P*<0.001, Table 2).

The retinas of normal subjects (Figure 4A) and unaffected G11778A mutation sibs (Figure 4B) were similar in

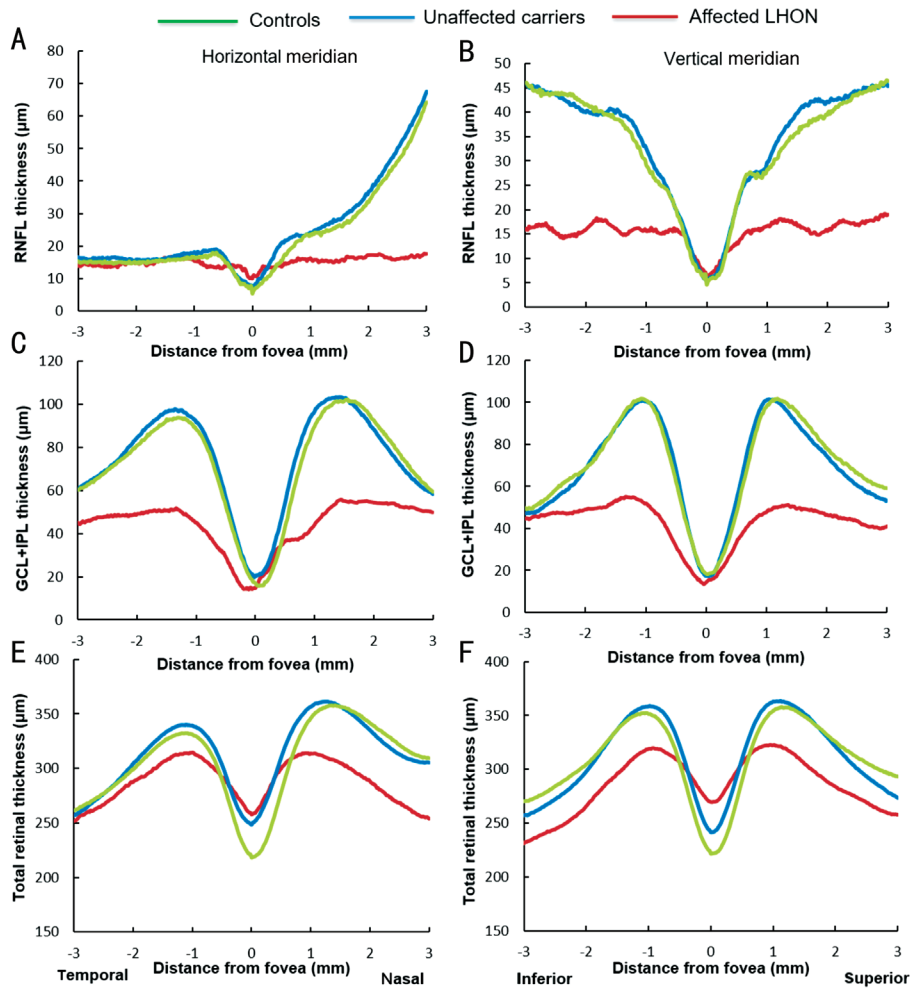


Figure 3 Thickness profiles of the RNFL, GCL+IPL, and total retina in controls, unaffected carriers, and affected LHON patients. Each thickness profile was constructed from the mean of all the subjects in each group and consisted of 300 data points. A: RNFL thickness profiles in the horizontal meridian; B: RNFL thickness profiles in the vertical meridian; C: GCL+IPL thickness profiles in the horizontal meridian; D: GCL+IPL thickness profiles in the vertical meridian; E: Total retinal thickness profiles in the horizontal meridian; F: Total retinal thickness profiles in the vertical meridian.

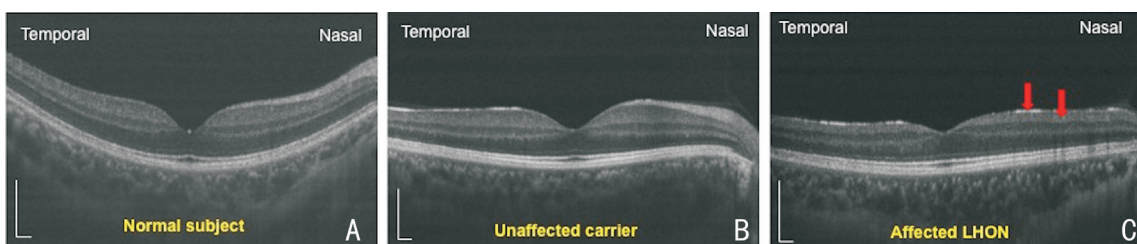


Figure 4 Representative retinal images of a control, an unaffected carrier, and an affected LHON patient taken by RTVue100 OCT. A: Normal retina; B: Unaffected retina of a G11778A carrier; C: Affected retina of an LHON patient. Red arrows: Thinner RNFL and GCL+IPL.

appearance. However, the RNFL and the GCL+IPL were markedly thinner in patients affected by LHON (Figure 4C). Both the RNFL and the GCL+IPL in affected LHON patients were thinner than in control subjects (both $P < 0.001$, Table 3). Additionally, the total retinal thickness in affected LHON patients was significantly thinner than that in the control group ($P = 0.009$). In affected LHON patients, the RNFL and total retinal thicknesses were significantly thinner in inferior, superior, and nasal sectors, but not in the temporal sector

(Figures 3, 5). The GCL+IPL in LHON patients was thinner in all sectors. There were no significant changes in the thickness of the other six intra-retinal layers in affected LHON patients or in unaffected carriers compared to control subjects (Table 3). Compared to normal subjects, the RNFL of affected LHON patients had more substantial decreases in thickness than did the GCL+IPL in all sectors except the temporal sector (Figure 6). The average decrease of RNFL for all sectors was 38.0%, and for the GCL+IPL, the average decrease was 40.1%.

Foveal pit morphological changes of LHON

Table 3 Macular intra-retinal layer thicknesses in the controls, unaffected carriers, and affected LHON patients mean±SD, μm

Layers	Controls	Unaffected carriers	Affected LHON	<i>P</i> (ANOVA)	<i>P</i> (LSD_1/2)	<i>P</i> (LSD_1/3)	<i>P</i> (LSD_2/3)
RNFL	27.66±2.12	29.02±2.92	15.48±3.93	<0.001	0.128	<0.001	<0.001
GCL+IPL	71.04±6.11	71.71±4.21	42.55±6.28	<0.001	0.689	<0.001	<0.001
INL	34.30±3.07	33.52±3.80	36.33±4.50	0.164	0.493	0.174	0.058
OPL	24.28±1.58	25.69±2.63	24.17±1.56	0.127	0.084	0.093	0.072
ONL	65.38±5.69	61.95±5.58	62.93±6.81	0.326	0.141	0.388	0.716
IS	21.41±1.24	23.70±3.93	22.57±6.45	0.170	0.061	0.447	0.460
OS	35.37±2.46	37.91±7.02	36.91±9.29	0.389	0.173	0.597	0.733
RPE	28.44±2.26	27.03±4.46	27.47±7.49	0.592	0.313	0.592	0.805
Total	307.88±16.06	312.44±19.69	287.09±22.83	0.005	0.440	0.009	0.001

RNFL: Retinal nerve fiber layer; GCL+IPL: Ganglion cell layer and inner plexiform layer; INL: Inner nuclear layer; OPL: Outer plexiform layer; ONL: Outer nuclear layer; IS: Inner segment; OS: Outer segment; RPE: retinal pigment epithelium; LSD_1/2: Fisher's least significant difference *t*-test between controls and unaffected carriers; LSD_1/3: Fisher's least significant difference *t*-test between controls and affected LHON patients; LSD_2/3: Fisher's least significant difference *t*-test between unaffected carriers and affected LHON patients.

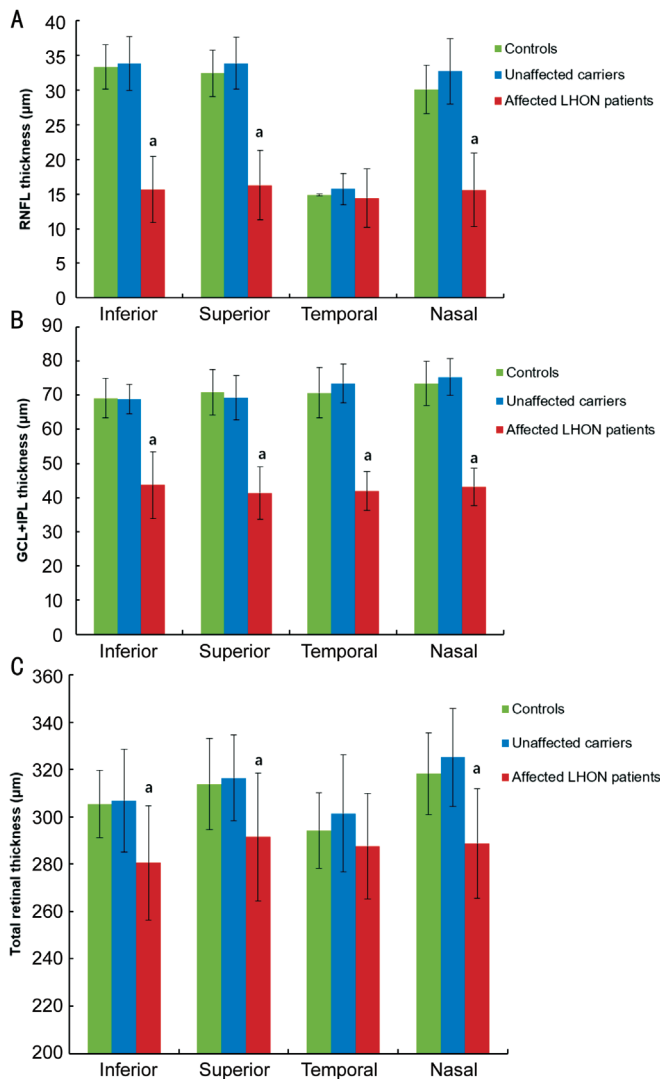


Figure 5 RNFL, GCL+IPL, and total retinal thicknesses in controls, unaffected carriers, and affected LHON patients by sectors A: RNFL; B: GCL+IPL; C: Total retina. ^a $P < 0.05$ compared to control subjects.

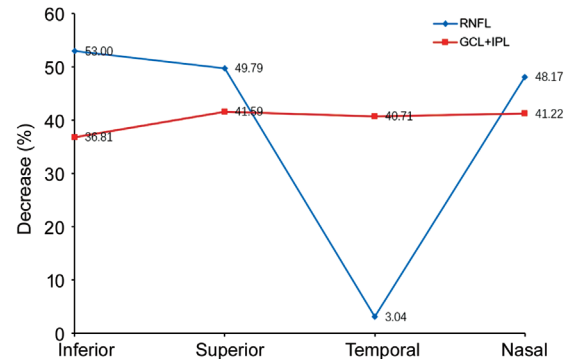


Figure 6 Percent decrease in thickness of the RNFL and GCL+IPL in affected LHON patients compared with controls Sector-specific decreases are shown.

DISCUSSION

The present study shows, for the first time, changes in the foveal pit morphology in both unaffected carriers and LHON patients from a family with the G11778A mutation. The foveal slopes in the temporal, nasal, inferior, and superior sectors were all flatter in both unaffected carriers and LHON patients. Further, the slopes of all four sectors in the LHON were flatter than those in the unaffected carriers. The average thicknesses of the RNFL, GCL+IPL, and total retina were thinner in the affected LHON patients compared to those in the unaffected carriers. Above all, the foveal pit morphology parameters may help distinguish the unaffected LHON-carriers with the G11778A mutation from a normal family member.

In our study, we found that the foveal morphology in unaffected carriers differed from the control subjects in that the pit depth and pit slope were smaller than in the normal controls. Although the unaffected carriers have a normal visual ability, the retinal structure and visual function have changed, which has also been reported in previous studies.

Soldath *et al*^[24] used OCT to evaluate the peripapillary RNFL thickness in unaffected carriers with LHON mutation. They found an increased RNFL thickness in the temporal sector in females with the G11778A mutation. Nikoskelainen *et al*^[11,27] observed, *via* fundus examination, peripapillary microangiopathy in unaffected carriers and characterized these patients as “mildly affected.” Sadun *et al*^[28] later confirmed this result. Additionally, Ziccardi *et al*^[9] reported that the 15’ pattern electroretinogram (PERG) P50-N95 amplitude in unaffected carriers was significantly reduced compared to controls. These results suggest that the structure changes may help distinguish unaffected carriers from normal subjects.

We found that the average thickness of the RNFL and the GCL+IPL in affected LHON patients was thinner than in the normal control group. The same observations were made for LHON patients by Barboni *et al*^[22], who evaluated the peripapillary RNFL thickness using a Stratus OCT instrument. Thirty-eight early and atrophic LHON patients were analyzed in their study, and the atrophic eyes had a thinner RNFL in all the measured sectors. Moreover, the RNFL structural abnormality was correlated with the functional defects in the affected LHON patients^[9,29]. Ziccardi *et al*^[9] found that the visual evoked potential (VEP) amplitudes were reduced, and the implicit times were significantly delayed when large (60’) and small (15’) check stimulations were used. Similar results were reported by Lam *et al*^[29] who found severe reductions in the PERG amplitude, which was associated with reduced visual acuity and severe visual field loss in the LHON patients. Further, microanatomy and histochemical studies showed ganglion cell death and optic nerve fiber degeneration in the LHON patients^[30], as also reported in neuropathological studies^[31]. Based on these observations, we suggest that the thinning of the RNFL and GCL+IPL is associated with visual function damage.

The thinner macula RNFL thickness in affected LHON patients mainly occurred in the nasal, inferior, and superior areas. The temporal side was less affected, possibly because, in normal subjects, the thickness of the temporal macular RNFL is less than that of the other sectors. Therefore, the temporal side may not be sensitive to LHON-induced changes. Another reason may be that the papillomacular bundle is smaller on the temporal side. As previously shown, the papillomacular bundle is the main target in the degenerative process of LHON^[24] because the small-caliber fibers are located in the nerve belonging to the parvocellular component of the RGCs. In addition, the RGCs are less myelinated, have the highest firing rate, and are thought to be very energy dependent. Therefore, they are the most susceptible to disruption of mitochondrial complex I activity^[30]. This might also explain why the average percent thickness decrease of the GCL+IPL in affected LHON

patients is more significant than for the RNFL.

The structural changes in our affected LHON patients mainly occurred in the RNFL and GCL+IPL. The outer retinal layers, such as the IS, OS, RPE, *etc.*, did not have any significant changes. These data suggest that the poor vision and severe visual field loss in affected LHON patients are due, at least in part, to the dysfunction of RGCs, which are not directly associated with the outer retinal layers. This hypothesis was validated by the PERG and VEP study of Ziccardi *et al*^[9]. This is also consistent with a histological study that found that the photoreceptors and RPE were spared in affected LHON patients^[32].

The main limitation of this study is the small number of LHON patients due to the low incidence of this disease in the general population. All the patients in our study were from a single-family and thus had the same point mutation. Because there were only four male and one female affected patients, statistical comparison of the foveal morphological parameters between the sexes could not be made. Another limitation is that the retinal images taken and analyzed were only in the horizontal and vertical meridians. In future studies, three-dimensional OCT scans and analyses will be more helpful in understanding the disease changes. These studies could also include longitudinal follow-up that may provide a greater understanding of the development of LHON. There were limitations of OCT in detecting affected and unaffected subjects as compared to controls due to the significant overlap of values among the 3 groups. Although in our study, we found no overlap in thickness between the affected LHON subjects compared to the unaffected and control subjects in some sections of RNFL and GCL+IPL. Due to the limited number of subjects and severe degree of LHON in our study, further study into identifying these distinguishing factors is required.

In conclusion, the foveal pit depth and pit slope were smaller in both unaffected carriers with the G11778A mutation and affected LHON patients than in controls. RNFL and GCL+IPL were thinner in affected LHON patients but not in unaffected carriers.

ACKNOWLEDGEMENTS

Foundation: Supported by Wenzhou Technology Program (No.Y20160148).

Conflicts of Interest: Liu XT, None; Shen MX, None; Chen C, None; Huang SH, None; Zhuang XR, None; Ma QK, None; Chen Q, None; Lu F, None; Yuan YM, None.

REFERENCES

- 1 Newman NJ, Bioussé V. Hereditary optic neuropathies. *Eye* 2004;18(11):1144-1160.
- 2 Chun BY, Rizzo JF 3rd. Dominant optic atrophy and leber’s hereditary optic neuropathy: update on clinical features and current therapeutic approaches. *Semin Pediatr Neurol* 2017;24(2):129-134.

- 3 Sadun AA, La Morgia C, Carelli V. Leber's hereditary optic neuropathy. *Curr Treat Options Neurol* 2011;13(1):109-117.
- 4 Manickam AH, Michael MJ, Ramasamy S. Mitochondrial genetics and therapeutic overview of Leber's hereditary optic neuropathy. *Indian J Ophthalmol* 2017;65(11):1087-1092.
- 5 Qu J, Wang Y, Tong Y, *et al.* Leber's hereditary optic neuropathy affects only female matrilineal relatives in two Chinese families. *Invest Ophthalmol Vis Sci* 2010;51(10):4906-4912.
- 6 Yen MY, Wang AG, Chang WL, Hsu WM, Liu JH, Wei YH. Leber's hereditary optic neuropathy the spectrum of mitochondrial DNA mutations in Chinese patients. *Jpn J Ophthalmol* 2002;46(1):45-51.
- 7 Guo H, Li S, Dai L, Huang X, Yu T, Yin Z, Bai Y. Genetic analysis in a cohort of patients with hereditary optic neuropathies in Southwest of China. *Mitochondrion* 2019;46:327-333.
- 8 Carelli V, Ross-Cisneros FN, Sadun AA. Mitochondrial dysfunction as a cause of optic neuropathies. *Prog Retin Eye Res* 2004;23(1):53-89.
- 9 Ziccardi L, Sadun F, De Negri AM, Barboni P, Savini G, Borrelli E, La Morgia C, Carelli V, Parisi V. Retinal function and neural conduction along the visual pathways in affected and unaffected carriers with Leber's hereditary optic neuropathy. *Invest Ophthalmol Vis Sci* 2013;54(10):6893-6901.
- 10 Salomão SR, Berezovsky A, Andrade RE, Belfort R Jr, Carelli V, Sadun AA. Visual electrophysiologic findings in patients from an extensive Brazilian family with Leber's hereditary optic neuropathy. *Doc Ophthalmol* 2004;108(2):147-155.
- 11 Nikoskelainen E, Hoyt WF, Nummelin K. Ophthalmoscopic findings in Leber's hereditary optic neuropathy. II. The fundus findings in the affected family members. *Arch Ophthalmol* 1983;101(7):1059-1068.
- 12 Mizoguchi A, Hashimoto Y, Shinmei Y, Nozaki M, Ishijima K, Tagawa Y, Ishida S. Macular thickness changes in a patient with Leber's hereditary optic neuropathy. *BMC Ophthalmol* 2015;15:27.
- 13 Kerrison JB, Howell N, Miller NR, Hirst L, Green WR. Leber hereditary optic neuropathy. Electron microscopy and molecular genetic analysis of a case. *Ophthalmology* 1995;102(10):1509-1516.
- 14 Lam BL, Burke SP, Wang MX, *et al.* Macular retinal sublayer thicknesses in G11778A leber hereditary optic neuropathy. *Ophthalmic Surg Lasers Imaging Retina* 2016;47(9):802-810.
- 15 Huang D, Swanson EA, Lin CP, *et al.* Optical coherence tomography. *Science* 1991;254:1178-1181.
- 16 Chiu SJ, Li XT, Nicholas P, Toth CA, Izatt JA, Farsiu S. Automatic segmentation of seven retinal layers in SDOCT images congruent with expert manual segmentation. *Opt Express* 2010;18(18):19413-19428.
- 17 Dubis AM, McAllister JT, Carroll J. Reconstructing foveal pit morphology from optical coherence tomography imaging. *Br J Ophthalmol* 2009;93(9):1223-1227.
- 18 Liu X, Shen M, Yuan Y, Huang S, Zhu D, Ma Q, Ye X, Lu F. Macular thickness profiles of intraretinal layers in myopia evaluated by ultrahigh-resolution optical coherence tomography. *Am J Ophthalmol* 2015;160(1):53-61.e2.
- 19 Wang Y, Jiang H, Shen M, *et al.* Quantitative analysis of the intraretinal layers and optic nerve head using ultra-high resolution optical coherence tomography. *J Biomed Opt* 2012;17(6):066013.
- 20 Pierro L, Iuliano L, Cicinelli MV, Casalino G, Bandello F. Retinal neurovascular changes appear earlier in type 2 diabetic patients. *Eur J Ophthalmol* 2017;27(3):346-351.
- 21 Ustaoglu M, Solmaz N, Onder F. Discriminating performance of macular ganglion cell-inner plexiform layer thicknesses at different stages of glaucoma. *Int J Ophthalmol* 2019;12(3):464-471.
- 22 Barboni P, Savini G, Valentino ML, *et al.* Retinal nerve fiber layer evaluation by optical coherence tomography in Leber's hereditary optic neuropathy. *Ophthalmology* 2005;112(1):120-126.
- 23 Barboni P, Carbonelli M, Savini G, Ramos Cdo V, Carta A, Berezovsky A, Salomao SR, Carelli V, Sadun AA. Natural history of Leber's hereditary optic neuropathy: longitudinal analysis of the retinal nerve fiber layer by optical coherence tomography. *Ophthalmology* 2010;117(3):623-627.
- 24 Soldath P, Wegener M, Sander B, Rosenberg T, Duno M, Wibrand F, Vissing J. Leber hereditary optic neuropathy due to a new ND1 mutation. *Ophthalmic Genet* 2017;38(5):480-485.
- 25 Newman NJ, Biousse V, Newman SA, Bhatti MT, Hamilton SR, Farris BK, Lesser RL, Turbin RE. Progression of visual field defects in leber hereditary optic neuropathy: experience of the LHON treatment trial. *Am J Ophthalmol* 2006;141(6):1061-1067.
- 26 Huang S, Chen Q, Ma Q, Liu X, Lu F, Shen M. Three-dimensional characteristics of four macular intraretinal layer thicknesses in symptomatic and asymptomatic carriers of g11778a mutation with leber's hereditary optic neuropathy. *Retina* 2016;36(12):2409-2418.
- 27 Nikoskelainen EK. Leber's hereditary optic neuroretinopathy, a maternally inherited disease. *Arch Ophthalmol* 1987;105(5):665.
- 28 Sadun AA, Salomao SR, Berezovsky A, *et al.* Subclinical carriers and conversions in Leber hereditary optic neuropathy: a prospective psychophysical study. *Trans Am Ophthalmol Soc* 2006;104:51-61.
- 29 Lam BL, Feuer WJ, Abukhalil F, Porciatti V, Hauswirth WW, Guy J. Leber hereditary optic neuropathy gene therapy clinical trial recruitment: year 1. *Arch Ophthalmol* 2010;128(9):1129-1135.
- 30 Howell N. Leber hereditary optic neuropathy: respiratory chain dysfunction and degeneration of the optic nerve. *Vision Res* 1998;38(10):1495-1504.
- 31 Yu-Wai-Man P, Votruba M, Burté F, La Morgia C, Barboni P, Carelli V. A neurodegenerative perspective on mitochondrial optic neuropathies. *Acta Neuropathol* 2016;132(6):789-806.
- 32 Carelli V, Sadun AA. Optic neuropathy in Lhon and Leigh syndrome. *Ophthalmology* 2001;108(7):1172-1173.